MOMENTUM COEFFICIENT AS A PARAMETER FOR AERODYNAMIC FLOW CONTROL WITH SYNTHETIC JETS

Sebastian D. Goodfellow
Mechanical and Industrial Eng.
University of Toronto
Toronto, Ontario, M5S 3G8, Canada
sebi.goodfellow@utoronto.ca

Serhiy Yarusevych
Mechanical and Mechatronics Eng.
University of Waterloo
200 University Avenue West
Waterloo, Ontario, N2L 3G1 Canada
syarus@uwaterloo.ca

Pierre E. Sullivan
Mechanical and Industrial Eng.
University of Toronto
Toronto, Ontario, M5S 3G8, Canada
sullivan@mie.utoronto.ca

ABSTRACT

The influence of periodic excitation from synthetic jet actuators, SJA, on boundary layer separation and reattachment over a NACA 0025 airfoil at a low Reynolds number is studied. All experiments were performed in a low-turbulence recirculating wind tunnel at a Reynolds number of $100,000$ and angle of attack of $\alpha = 5^\circ$. Mounted below the surface of the airfoil, the SJA consists of four (32.77mm diameter) piezoelectric ceramic diaphragms positioned in a single row. Initial flow visualization and hot–wire tests were conducted in quiescent environmental conditions to characterize the exit flow from the SJA. Flow visualization results showed a vertical jet pulse accompanied by two counter rotating vortices being produced at the exit of the simulated slot, with the vortices shed at the excitation frequency. Hot-wire measurements determined the maximum jet velocity for a range of excitation frequencies (f_e = 50Hz - 2.7kHz) and voltages ($V_{app} = 50 - 300V_{p-p}$), which were used to characterize the excitation amplitude in terms of the momentum coefficient (C_μ). With the SJA installed in the airfoil, flow visualization results showed a reattachment of the boundary layer and a significant reduction in wake width. Wake velocity profiles were obtained two chord lengths downstream of the trailing edge to assess the excitation effect on drag and wake characteristics. A spectral analysis was conducted in the wake region and showed the presence of vortex shedding at a frequency of 22 Hz. When excitation was applied at 935 Hz and 250 V_{p-p}, the shedding frequency shifted to 50Hz. The results suggest it is possible to get substantial improvement in airfoil performance at lower input power.

INTRODUCTION

Aerodynamic control of low Reynolds number flow using synthetic jet actuation is of interest to a wide range of applications including the design and operation of unmanned aerial vehicles (UAVs) at low speeds, separation control at the inlets of jet engines and the design of compressor blades.

Periodic excitation introduced locally at the surface has shown the most promise as an efficient and practical means of flow control. Much work has been done to identify optimum frequency ranges for producing reattachment of a separated shear layer using synthetic jets. There are two distinct frequency bands which have received the most attention. The first range includes the dominant wake frequency, otherwise known as the shedding frequency f_s, and the second range involves frequencies that are at least an order of magnitude higher than f_s. In their review, Greenblatt & Wygnanski (2000) found that, except for one, all studies showed an optimum dimensionless excitation frequency, F^+, range of $1 \leq F^+ \leq 2.5$, where $F^+ = f_e L/U_o$. In contrast, Amitay et al. (2001) found that dimensionless frequencies an order of magnitude higher than the natural shedding frequency are, in fact, more effective. Amitay et al. (2001) suggest that use of different excitation methods may be the cause for the drastically different results. When exciting flow over a frequency range of $0Hz \leq f_e \leq 1480Hz$ (Amitay & Glezer (2002, 2005); Amitay et al. (2001)), internally mounted audio speakers were used for $0Hz \leq f_e \leq 300Hz$ and compact piezoceramic actuators were used for $300Hz \leq f_e \leq 1480Hz$. For $f_e \leq 300Hz$, the jets driven by audio speakers were spanwise uniform but, for $f_e \geq 300Hz$, their performance was greatly reduced both in the presence and absence of crossflow. In fact, in the presence of crossflow, the jet velocity reduced by more than 80%, which greatly diminished performance. Therefore, a spanwise uniform piezoelectric actuator, with a small cavity tuned to high frequencies, was used for $f_e \geq 300Hz$.

Amitay & Glezer (2005) show that low frequency excitation, within the range of f_s, and high frequency excitation, an order of magnitude higher than f_s, have a distinctly

different effects on the separated shear layer. At excitation frequencies close to f_s, the separated shear layer is deflected towards the surface and a vortex trail can be seen advecting along the airfoil surface. These vortices persist well into the trailing edge region of the airfoil, being enhanced as they are advected downstream due to a possible coupling between the excitation frequency and the shedding frequency. At dimensionless frequencies at least an order of magnitude higher than f_s, the flow was fully attached to the surface of the airfoil and there was no sign of large–scale coherent structures. Amitay & Glezer (2005) suggest that the effect of high frequency excitation is the alteration of flow upstream of the separation point and ultimately a suppression or bypass of separation.

In addition to the excitation frequency, there are three important design parameters, namely, the excitation location, excitation amplitude and number of excitation jets (Amitay & Glezer (2002); Greenblatt & Wygnanski (2000); Glezer & Amitay (2002)). For the excitation location, it is suggested that excitation is more effective when introduced upstream of separation, but there are no consistent recommendations for the most effective placement of actuators. The findings of Amitay et al. (2001) illustrate the complexity of the problem when excitation frequency is introduced as a variable. With actuators located at the most upstream position and excitation applied at f_e = 246Hz and 740Hz, excitation had virtually no effect on the pressure distribution over the airfoil. On the other hand, actuators at the same position and excitation at f_e = 71Hz resulted in flow reattachment and the formation of a separation bubble. Investigating the effect of excitation amplitude with external acoustic excitation, Yarusevych et al. (2006) showed that C_L increases with increasing sound pressure level, but this increase is checked. The same trend was observed in studies involving synthetic jets, where the excitation amplitude is commonly characterized by the momentum coefficient, C_μ. The third design parameter is the number of synthetic jet actuators. In some earlier studies, only one synthetic jet was used (*e.g.,* Greenblatt & Wygnanski (2000)); Smith & Glezer (2002) showed that two adjacent and out of phase jets are more effective in the entrainment of free stream fluid for jet vectoring applications.

This paper studies the effect of input power (correlated to SJA exit velocity), excitation frequency of the SJA and input voltage on flow over an airfoil operating at at a Reynolds number of 100000 and angle of attack of 5° to show it is possible to minimize power requirements.

EXPERIMENTAL METHOD

The performance of a NACA0025 airfoil at a Reynolds number of $100,000$ and angle of attack, α, of 5^o was studied. The NACA 0025 airfoil has a chord length of 30cm and a thickness of 7.5cm, and was located 0.4m downstream of the contraction. All experiments were conducted in the low-turbulence recirculating wind tunnel in the Department of Mechanical and Industrial Engineering at the University of Toronto. The test section is 5 m long, 0.91 m wide and 1.22 m high and has a free stream turbulence intensity level less than 0.1%.

Piezo-electric actuators produced by Face International Corporation were used in the SJA. The piezo-electric actuators are driven by a high voltage amplifier with a gain of 100 and maximum output of $400V_{p-p}$ at 250 mA. The SJA was constructed of aluminum with a total cavity volume of approximately $677.6mm^3$. A pocket was milled out from the top of the airfoil to allow for the SJA to be mounted flush with the surface. The exit slot of the SJA measured 140mm × 0.5mm and was located 101mm downstream of the leading edge. Finite element analysis identified a natural frequency for the SJA at $935Hz$. Based on this, frequencies at $935Hz$ and above and below were used in this study. It was impossible to drive the actuators at $1870Hz$ and no appreciable effect was found at $420Hz$.

Flow velocity data were obtained with constant temperature anemometers (Dantec 56C01 main units equipped with 56C17 CTA bridges) and a Dantec 55P01 normal hot-wire probe. The anemometer was connected to a National Instruments 4472 24-bit digital acquisition board.

To visualize airfoil boundary layer development and wake formation, a smoke wire technique was employed. A smoke wire installed 10 cm upstream of the leading edge was coated with smoke-generator fluid. A thin 0.076 mm diameter 304 stainless steel wire was chosen in order to provide adequate smoke density, while not introducing appreciable disturbances into the flow field.

The synthetic jet was quantified using the momentum coefficient C_μ, as defined by Amitay et al. (2001).

$$C_\mu = \frac{\bar{I}_j}{\frac{1}{2}\rho_o U_o^2 c} \tag{1}$$

where $\overline{I_j}$ is the time-averaged jet momentum per unit length during the outstroke, ρ_o is the freestream fluid density, c is the chord, and U_o is the freestream velocity.

$$\bar{I}_j = \frac{1}{\tau}\rho_j b \int_0^\tau u_j^2(t)dt \tag{2}$$

where τ = T/2, T is the period of the diaphragm motion, ρ_j is the jet density, b is the jet orifice width, and $u_j(t)$ is the phase averaged velocity at the jet exit plane.

The airfoil drag was calculated based on the momentum integral defined by Equation 3 (Antonia & Rajagopalan (1990)), where Y_1 and Y_2 are the wake boundaries and $\bar{U}$ and U_o are the mean velocity in the wake region and the free stream velocity respectively.

$$C_d = \frac{2}{c}\int_{Y_1}^{Y_2} \frac{\bar{U}}{U_o}\left(1 - \frac{\bar{U}}{U_o}\right)dY \tag{3}$$

At each vertical position in the wake region, 100,000 datapoints were used to calculate average velocity.

Spectral analysis was performed to identify organized flow structures in the wake and determine their characteristics. For each spectrum, 2^{20} velocity data points were acquired in the wake at $X/c = 2$ and were then divided into 256 bins of 4096 data points. The autospectra of individual segments were computed and averaged.

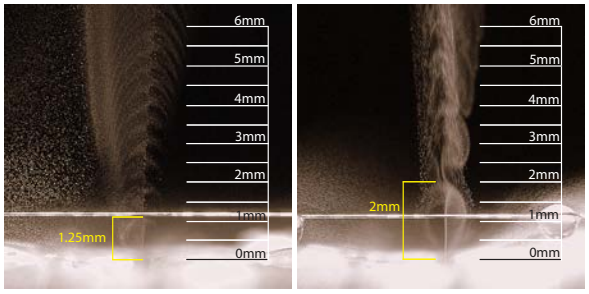

(a) f_e = 500Hz, $C_\mu = 1.45 \times 10^{-4}$ (b) f_e = 700Hz, $C_\mu = 5.68 \times 10^{-4}$

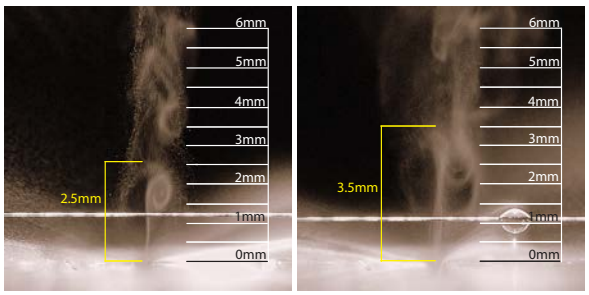

(c) f_e = 750Hz, $C_\mu = 9.06 \times 10^{-4}$ (d) f_e = 800Hz, $C_\mu = 1.62 \times 10^{-3}$

Figure 1: Flow visualization at the slot exit

SYNTHETIC JET ACTUATOR CHARACTERIZATION

Images were taken at excitation frequencies, f_e= 500, 700, 750 and 800Hz for an applied voltage, V_{app}, of 200V_{p-p}. Figure 1 shows flow visualization images obtained with the smoke wire positioned perpendicular to the exit slot and centred at the piezo-electric diaphragm. When the SJA is run at an excitation frequency of 500Hz, small jet pulses accompanied by two counter rotating vortices are produced (Figure 1a). As the excitation frequency is increased to 800Hz, the vortex length increases from roughly 1.25mm to approximately 3.5mm. It was not possible to obtain good images at higher excitation frequencies. Smith & Swift (2003), Zhong et al. (2007), Zhang & Tan (2007), Holman et al. (2005) and Yang (2009) observed similar counter–rotating vortices formed by a synthetic jet.

Hot–wire measurements were taken at the jet exit plane with the wire positioned parallel to the slot. The velocity data were phase averaged over a full 360^o period of the piezo-electric diaphragms. Figure 2 shows the variation of the jet velocity during the operation cycle for f_e = 935 Hz, C_μ = 1.21×10^{-2}. The peak expulsion velocity is 16.65 m/s at ϕ = 100^o and the peak ingestion velocity is -16.65 m/s at ϕ = 275^o.

For f_e = 935 Hz, $V_{app} = 275V_{p-p}$ (Figure 2), the minimum velocity is 3 m/s meaning that as the position of the diaphragm changes from the expulsion to the ingestion part of the cycle, the fluid never reaches a zero velocity across the inlet. Mane et al. (2008) found a zero velocity was reached between the expulsion and ingestion. Here, the expulsion and ingestion peaks are roughly of the same magnitude, but the results of Mane et al. (2008) show an ingestion peak that is less than half the magnitude of the expulsion peak. This is likely because our measurements were taken at the jet exit plane while the measurements of Mane et al. (2008) were

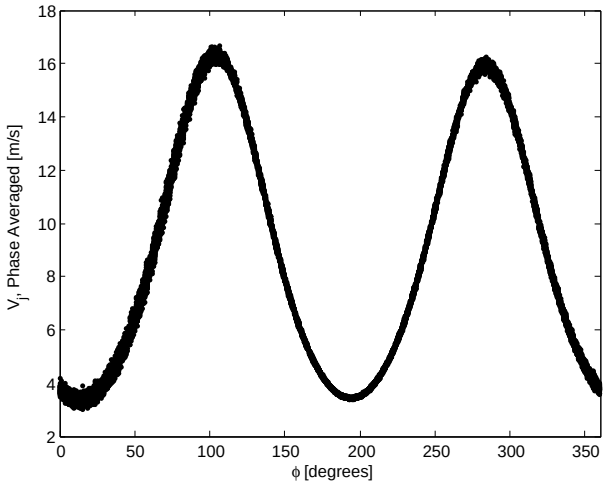

Figure 2: Phase averaged jet velocity profile for f_e = 935Hz and $C_\mu = 1.21 \times 10^{-2}$

taken 2mm away from the exit plane. Studies were conducted to describe velocity profile evolution as the hotwire probe was moved away from the slot. When comparing measurements taken at the slot exit to those taken 3mm away, we found that the expulsion peak had diminished slightly but the ingestion peak was roughly half the magnitude of the expulsion peak. These results show that flow ingestion occurs close to the exit plane and it is essential to measure at the exit plane to correctly characterize the synthetic jet.

RESULTS

Mean Velocity Profiles The synthetic jet actuator was installed in the NACA 0025 airfoil and placed in the windtunnel. The SJA was positioned at the exit slot just upstream of the separation point.

Mean velocity profiles were obtained by traversing the airfoil wake in the Y - direction at a position two chords downstream from the trailing edge (X/c = 2). The origin of the coordinate system used for the wake velocity profiles is at the trailing edge of the airfoil, with the Y - axis perpendicular to the streamwise direction and the X - axis is pointing downstream. Figure 3a shows the mean wake velocity profile corresponding to the uncontrolled case. Figures 3b – 3d show the wake width and the maximum velocity deficit decrease with increasing C_μ.

Flow Visualization A series of flow visualizations were conducted with the smoke wire in the upstream position (10cm from the leading edge) and centered along the length of the SJA slot in the Z - direction. Figures 4 and 5 show the uncontrolled and controlled wake extending roughly 3 chord lengths downstream. Figure 4 shows the presence of boundary layer separation on the upper surface without subsequent reattachment and large scale coherent structures forming in the wake. When excitation is applied at f_e = 935 Hz, at the maximum C_μ considered here, 1.2×10^{-2} and V_{app} = 275 V_{p-p} (Figure 5), boundary layer separation on the upper surface is suppressed and the wake width is reduced substantially similar to that seen by Yarusevych et al. (2007).

Spectral Analysis Figure 6 shows the drop in drag co-

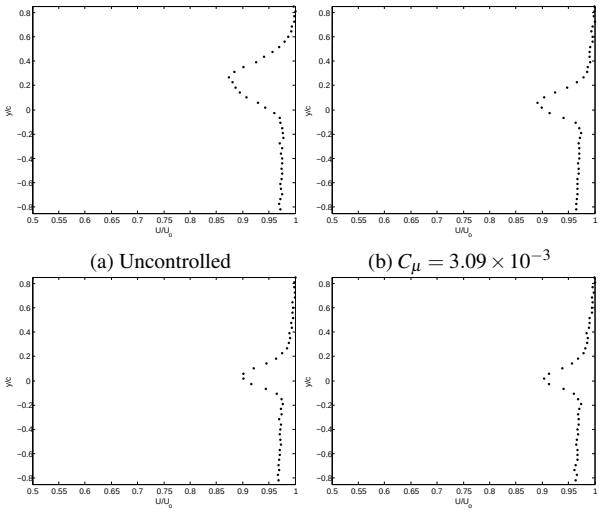

(a) Uncontrolled (b) $C_\mu = 3.09 \times 10^{-3}$

(c) $C_\mu = 6.76 \times 10^{-3}$ (d) $C_\mu = 1.0 \times 10^{-2}$

Figure 3: Mean wake velocity profiles for $Re_c = 100 \times 10^3$ at $\alpha = 5^o$, $f_e = 935$Hz

efficient (C_d) for increasing momentum coefficient, (C_μ), for a constant excitation frequency of 935Hz. As C_μ increased from 0 to 1.56×10^{-3}, there is no significant change in C_d, but when C_μ is further increased to 3.09×10^{-3}, C_d decreases to 0.036. When C_μ is 6.76×10^{-3} the drag coefficient drops to 0.0276. Increasing C_μ further past 6.76×10^{-3} has no significant effect ondrag. The total drag reduction in this study was about 66%.

Wake velocity spectra obtained at $X/c = 2$ and f_e = 935Hz (Figure 7) suggest that characteristics of wake structures change significantly with increasing C_μ. Without excitation, a peak occurs in the spectra at 22Hz, with an energy level of roughly 3.0×10^4, and is attributed to the shedding of large scale structures in the wake. When excitation is introduced at C_μ =3.23×10^{-4} and 1.56×10^{-3}, there is no appreciable effect on the spectrum. When C_μ is increased to 3.09×10^{-3}, the spectral peak at f = 22Hz is flattened out. This flattening of the spectral peak at f = 22Hz corresponds to a 52% reduction in drag. When C_μ reaches 6.76×10^{-3}, the low frequency spectral energy level drops slightly, which corresponds to another 11% drop in C_d. As mentioned above, increasing C_μ further past 6.76×10^{-3} has no significant effect on airfoil performance. For $C_\mu = 1.0 \times 10^{-2}$, there is a new spectral peak at 50Hz. Airfoil performance is not enhanced because the wake geometry does not change, see *e.g.,* the mean velocity profiles for $C_\mu = 6.76 \times 10^{-3}$ and $C_\mu = 1.0 \times 10^{-2}$ (Figures 3c and 3d).The results show that increasing C_μ eventually causes the wake frequency to "lock in" on a particular value ($50Hz$ in the present study). Substantial energy is required to trigger this "lock in" effect, but practically, this is not beneficial as there is no appreciable change in the wake width.

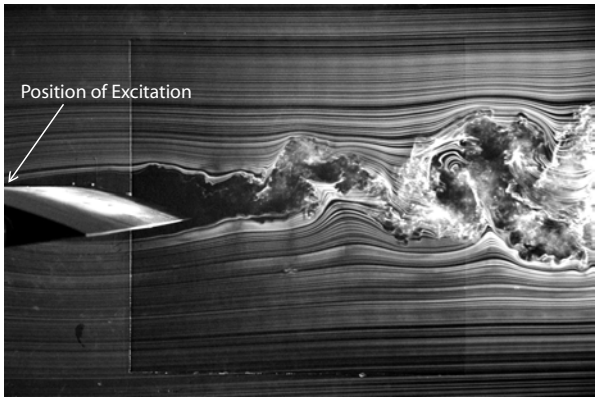

Figure 4: Flow visualization at $Re_c = 100 \times 10^3$ and α = 5^o with a single upstream smoke wire. Uncontrolled (Separated Boundary Layer)

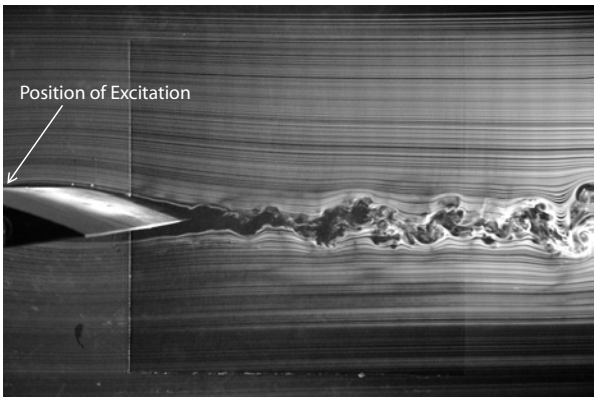

Figure 5: Flow visualization at $Re_c = 100 \times 10^3$ and $\alpha = 5^o$ with a single upstream smoke wire. Controlled (Reattached Boundary Layer), f_e = 935Hz, $C_\mu = 1.24 \times 10^{-2}$

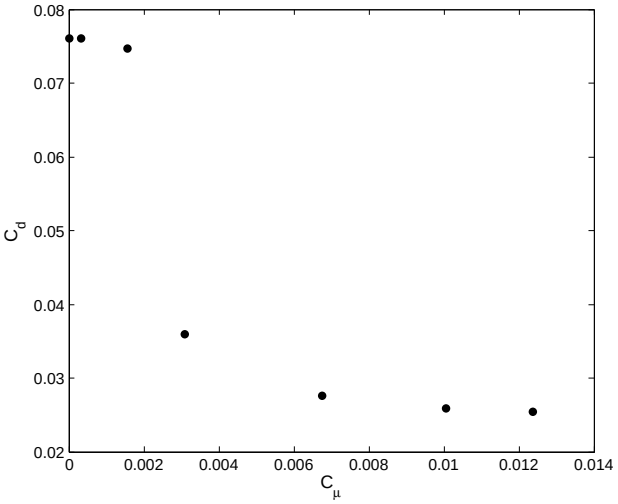

Figure 6: Drag coefficient, C_d, at $\alpha = 5^o$ for $Re_c = 100 \times 10^3$ and f_e = 935Hz for increasing C_μ

To confirm the presence of dominant coherent structures in the wake as a result of the "lock in" effect, flow visualization images were analyzed. Figure 8 shows flow visualization at f_e = 935Hz for $C_\mu = 1.56 \times 10^{-3}$, 3.09×10^{-3}, 6.76×10^{-3} and 1.0×10^{-2}. Figure 8a is at the conditions where there is a dominant spectral peak at f = 22Hz and Figure 8b corresponds

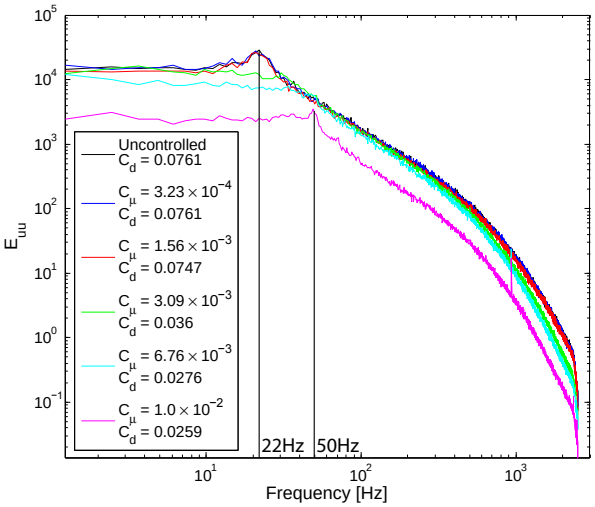

Figure 7: Spectra of the streamwise fluctuating velocity component at $X/c = 2$ and $\alpha = 5^o$ for $Re_c = 100 \times 10^3$ and $f_e = 935$Hz

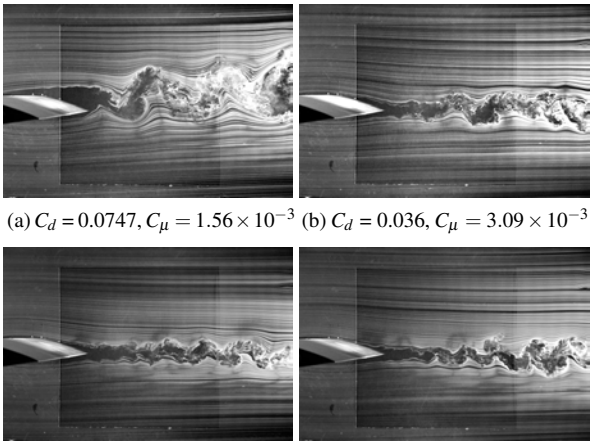

(a) $C_d = 0.0747$, $C_\mu = 1.56 \times 10^{-3}$ (b) $C_d = 0.036$, $C_\mu = 3.09 \times 10^{-3}$

(c) $C_d = 0.0276$, $C_\mu = 6.76 \times 10^{-3}$ (d) $C_d = 0.0259$, $C_\mu = 1.0 \times 10^{-2}$

Figure 8: Flow visualization at $Re_c = 100 \times 10^3$ and $\alpha = 5^o$ with a single upstream smoke wire for $f_e = 935$Hz

to the conditions which cause flattening of that peak and is an example of the flow typically seen in this case.The wake is smaller in the vertical direction which results in a smaller C_d, and the large scale vortices in the wake are replaced by weaker, smaller-scale coherent structures. Figure 8b corresponds to the green spectrum in Figure 7. Indeed, there is no peak at $22Hz$. However, there is a smaller magnitude peak at about $30Hz$ in the green spectrum. This, suggests that there are smaller scale coherent structures in the wake that are less organized than those in Figure 8a. Maximum drag reduction is achieved in achieved in Figure 8c ($C_\mu = 6.76 \times 10^{-3}$, C_d = 0.0276) where the boundary layer has been reattached and the wake size in the vertical direction has reached a minimum. The spectrum (Figure 7) shows a broad peak emerging at $50Hz$. Figure 8d ($C_\mu = 1.0 \times 10^{-2}$, C_d = 0.0259) does not show any further reduction in wake size, but the structures within the wake do appear to be more ordered which agrees with the emergence of a spectral peak at $50Hz$ in the velocity spectrum (Figure 7).

Figure 9 is C_μ plotted for various excitation frequency and applied voltage combinations. The main data set shown with correspond to holding input voltage constant at $275V_{p-p}$ and varying f_e from 450Hz - 1200Hz. The points located at f_e = 935Hz corresponds to applied voltages of 100, 150, and $200V_{p-p}$. Data points of the same color have a similar C_μ where these colors correspond to the colors in Figure 10. Yarusevych et al. (2009) demonstrated that excitation frequency was a crucial input parameter for flow control using external acoustic excitation and we are now interested in knowing if this also the case for local periodic excitation. When C_μ is roughly the same but f_e is different we would expect to see the same wake spectra if f_e is not a controlling input parameter.

Figure 10 shows spectra obtained at several excitation frequencies corresponding to all the colored points in Figure 9. Straight and dashed lines of the same color correspond to a different f_e but roughly the same C_μ. It is clear that excitation frequency must play an important role because in most cases the spectra are drastically different for a similar C_μ. For

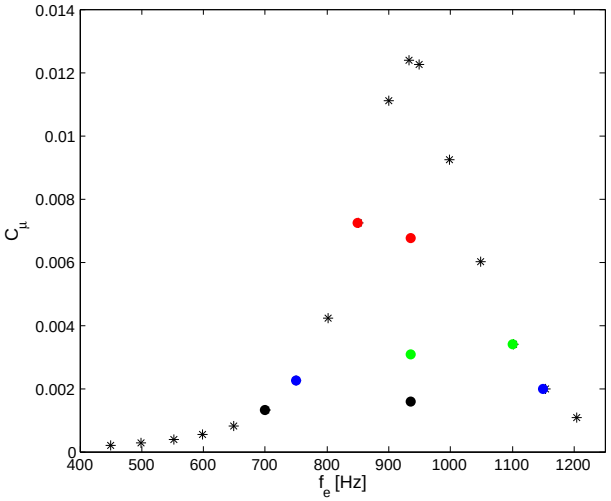

Figure 9: Momentum Coefficient, C_μ, for f_e = 450Hz - 1200Hz and $V_{app} = 275V_{p-p}(*)$

$C_\mu = 1.56 \times 10^{-3}$, f_e = 935Hz (—) and $C_\mu = 1.33 \times 10^{-3}$, f_e = 700Hz (- -) the higher excitation frequency does not have any effect on the flow given that a spectral peak at $22Hz$ is present. When holding C_μ at roughly the same level but decreasing f_e to 700Hz, the spectral peak at $22Hz$ disappears. Wake measurements (not presented here) showed this is accompanied by a drag reduction of about 66%. This effect is repeated when looking at the the green and red data points. Where C_μ is held constant, f_e = 935Hz is always less effective than 700Hz (black), 850Hz (red) and 1100Hz (green). When comparing two excitation treatments where C_μ is the same and the excitation frequencies are different but not equal to 935Hz (blue), f_e does not play a role. For f_e = 750Hz and 1150Hz (blue) wake spectra are comparable to the results for successful control at $935Hz$. The result suggest that the transition mechanism at $935Hz$ (the natural frequency of the SJA) is gradual when compared to that of the other f_e considered where the switch from one state to the other was immediate.

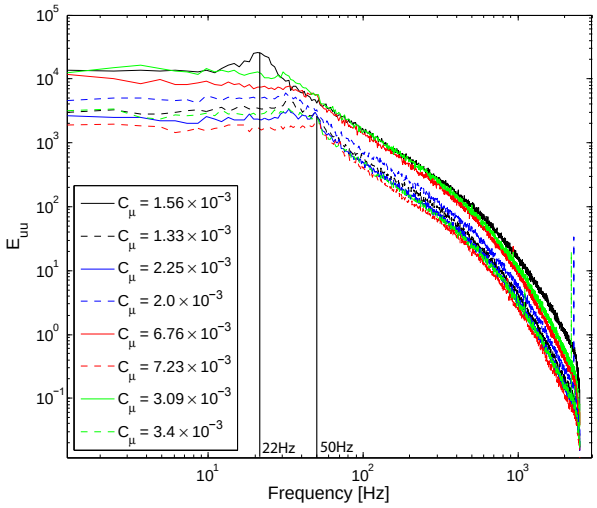

Figure 10: Spectra of the streamwise fluctuating velocity component at $X/c = 2$ and $\alpha = 5^o$ for $Re_c = 100\times10^3$ and f_e = 935Hz(—), f_e = 700Hz(- -), f_e = 750Hz(—), f_e = 1150Hz(- -), f_e = 935Hz(—), f_e = 850Hz(- -), f_e = 935Hz(—), f_e = 1100Hz(- -)

CONCLUSION

A Synthetic Jet Actuator and its effect on the separated shear layer and wake of a NACA 0025 airfoil have been studied experimentally. Wind tunnel tests were then conducted for a Reynolds numbers of 100,000 and angle of attack of 5^o.

The SJA was first characterized in quiescent flow and was found computationally and experimentally to have a resonant frequency of 935 Hz. The maximum attainable jet velocity is 16.7 m/s for f_e = 935Hz and $V_{app} = 275V_{p-p}$. It was shown that the jet velocity and momentum coefficient increase with an increase in applied voltage. When excitation was applied at f_e = 935 Hz and C_μ = 0.0121, the boundary layer reattached and the wake width was reduced significantly. However, substantial drag reduction was possible at lower frequencies and voltages. Drag reduction was correlated to C_μ; however, the mechanism differed and was dependent on f_e. At the natural frequency of the SJA, there was a gradual transition from one wake condition to another. At other f_e near this critical value, the transition was abdrupt. This suggests it is possible to perform effective aerodynamic control at lower input power. The results also show that excitation alters characteristics of wake coherent structures, increasing their characteristic frequency and reducing the energy content.

References

Amitay, M., & Glezer, A. (2002). Role of Actuation Frequency in Controlled Flow Reattachment over a Stalled Airfoil. *AIAA Journal*, *40*, 209–216.

Amitay, M., & Glezer, A. (2005). Aspects of Low - and high - Frequency Actuation for Aerodynamic Flow Control. *AIAA Journal*, *43*, 1501–1511.

Amitay, M., Smith, D., Kibens, V., Parekh, D. E., & Glezer, A. (2001). Aerodynamic Flow Control over and Unconventional Airfoil Using Synthetic Jet Actuators. *AIAA Journal*, *39*, 361–370.

Antonia, R., & Rajagopalan, S. (1990). Determination of Drag of a Circular Cylinder. *AIAA Journal*, *28*, 1833–1834.

Glezer, A., & Amitay, M. (2002). Synthetic Jets. *Annu, Rev. Fluid Mech*, *34*, 503–529.

Greenblatt, D., & Wygnanski, I. J. (2000). The Control of Flow Separation by Periodic Excitation. *Progress in Aerospace Sciences*, *36*, 487–545.

Holman, R., Utturkar, Y., R, Mittal, Smith, B. L., & Cattafesta, L. (2005). Formation Criterion for Synthetic Jets. *Science in China Series E: Technological Sciences*, *43*, 2110–2116.

Mane, P., Mossi, K., & Bryant, R. (2008). Synthetic Jets. *Smart Materials and Structures*, *17*, 1–12.

Smith, B., & Glezer, A. (2002). Jet Vectoring using Synthetic Jets. *J. Fluid Mech*, *458*, 1–34.

Smith, B., & Swift, G. (2003). A Comparison Between Synthetic Jets and Continuous Jets. *Experiments in Fluids*, *34*, 467–472.

Yang, A. (2009). Design analysis of a piezoelectrically driven synthetic jet actuator. *Smart Materials and Structures*, *18*, 1–12.

Yarusevych, S., Kawall, J. G., & Sullivan, P. E. (2006). Airfoil performance at low Reynolds numbers in the presence of periodic disturbances. *Journal of Fluids Engineering, Transactions of the ASME*, *128*(3), 587–595.

Yarusevych, S., Sullivan, P. E., & Kawall, J. G. (2007). Effect of acoustic excitation amplitude on airfoil boundary layer and wake development. *AIAA Journal*, *45*(4), 760–771.

Yarusevych, S., Sullivan, P. E., & Kawall, J. G. (2009). On Vortex Shedding from an Airfoil in Low-Reynolds-Number Flows. *J. Fluid Mech*, *632*, 1–27.

Zhang, J., & Tan, X. (2007). Experimental Study on Flow and Heat Transfer Characteristics of Synthetic Jet Driven by Piezoelectric Actuator. *Science in China Series E: Technological Sciences*, *50*, 221–229.

Zhong, S., Jabbal, M., Tang, H., Garcillan, L., Guo, F., Wood, N., et al. (2007). Towards the Design of Synthetic - jet Actuators for Full-scale Flight Conditions. Part 1: The Fluid Mechanics of Synthetic-jet Actuators. *Experiments in Fluids*, *78*, 283–307.